

Geophysical Research Letters[®]



RESEARCH LETTER

10.1029/2023GL105307

Key Points:

- A new ice-core based reconstruction of volcanic sulfate in the atmosphere (1733–1895) includes small-to-moderate eruptions
- Small-to-moderate eruptions can induce significant surface cooling and help explain the long-lasting cooling in the early 19th century
- Regional cooling from small-to-moderate eruptions may be influenced by the circulation changes from the 1815 Tambora for over 10 years

Supporting Information:

Supporting Information may be found in the online version of this article.

Correspondence to:

S.-W. Fang,
shih-wei.fang@mpimet.mpg.de

Citation:





Fang, S.-W., Sigl, M., Toohey, M., Jungclauss, J., Zanchettin, D., & Timmreck, C. (2023). The role of small to moderate volcanic eruptions in the early 19th century climate. *Geophysical Research Letters*, 50, e2023GL105307. <https://doi.org/10.1029/2023GL105307>

Received 11 JUL 2023
Accepted 23 OCT 2023

© 2023. The Authors.

This is an open access article under the terms of the [Creative Commons Attribution-NonCommercial-NoDerivs License](https://creativecommons.org/licenses/by-nc-nd/4.0/), which permits use and distribution in any medium, provided the original work is properly cited, the use is non-commercial and no modifications or adaptations are made.

The Role of Small to Moderate Volcanic Eruptions in the Early 19th Century Climate

Shih-Wei Fang¹ , Michael Sigl^{2,3}, Matthew Toohey⁴, Johann Jungclauss¹ , Davide Zanchettin⁵ , and Claudia Timmreck¹ 

¹Max-Planck-Institut für Meteorologie, Hamburg, Germany, ²Department of Climate and Environmental Physics, University of Bern, Bern, Switzerland, ³Oeschger Centre for Climate Change Research, Bern, Switzerland, ⁴University of Saskatchewan, Saskatoon, SK, Canada, ⁵University Ca' Foscari of Venice, Venezia, Italy

Abstract Small-to-moderate volcanic eruptions can lead to significant surface cooling when they occur clustered, as observed in recent decades. In this study, based on new high-resolution ice-core data from Greenland, we produce a new volcanic forcing data set that includes several small-to-moderate eruptions not included in prior reconstructions and investigate their climate impacts of the early 19th century through ensemble simulations with the Max Planck Institute Earth System Model. We find that clustered small-to-moderate eruptions produce significant additional global surface cooling (~ 0.07 K) during the period 1812–1820, superposing with the cooling by large eruptions in 1809 (unidentified location) and 1815 (Tambora). This additional cooling helps explain the reconstructed long-lasting cooling after the large eruptions, but simulated regional impacts cannot be confirmed with reconstructions due to a low signal-to-noise ratio. This study highlights the importance of small-to-moderate eruptions for climate simulations as their impacts can be comparable with that of solar irradiance changes.

Plain Language Summary Volcanic eruptions can influence global climate through the emission of sulfuric acids shielding Earth from incoming solar radiation. Previous volcanic reconstructions based on ice-cores from the polar regions, however, only considered very strong volcanic eruptions. In this study, based on new ice-core measurements from Greenland, we reconstruct for the first time volcanic sulfur emissions from small to medium-sized eruptions and investigate their impact on climate in the early 19th century through experiments with the Max Planck Institute Earth System Model (MPI-ESM1.2-LR). We find that clustering of small to medium-sized eruptions can cause significant global surface cooling (~ 0.07 K), which during the 1812–1820 period amplified the cooling caused by the two known large eruptions of the period (1809 unidentified and 1815 Tambora). This additional surface cooling from small eruptions helps explain the long-lasting cooling after the two strong eruptions generally found in the reconstruction, but the simulated regional impacts cannot be fully confirmed with reconstructions that are too noisy. This study highlights the importance of including small-to-moderate eruptions for climate model simulations as their impacts are comparable with that of solar irradiance forcing.

1. Introduction

The early 19th century, with the final resurgence of the Little Ice Age, represents the coldest period of the past 500 years (PAGES 2k Consortium, 2019; Reichen et al., 2022; Wanner et al., 2022), best illustrated by the widespread advance of alpine glaciers (Solomina et al., 2016). The cold climate over this period is believed to be caused mainly by sulfuric aerosol enhancements resulting from strong tropical volcanic eruptions, including the widely known 1815 Tambora eruption and the unidentified 1809 eruption suspected to have occurred in the tropics (Brönnimann, Franke, et al., 2019; Cole-Dai et al., 2009; Sigl et al., 2018; Timmreck et al., 2021). However, with model simulations, these two strong eruptions alone cannot explain the cold surface anomalies reconstructed and observed during the decade between 1810 and 1820, especially the long-lasting post-volcanic cooling after each of the two eruptions (Timmreck et al., 2021). Besides the two strong eruptions, lower solar radiation co-existed in the period, the so-called Dalton grand solar minimum (1797–1823; Brehm et al., 2021). Zanchettin et al. (2013) and Anet et al. (2014) have argued that the coinciding lower solar irradiance is crucial for explaining the early 19th century cooling, especially the long-lasting cooling after the eruptions, while others have argued for limited contributions of solar irradiance changes (Fang et al., 2022; Owens et al., 2017; Schurer et al., 2014).

Even if models correctly represent the cooling from the solar irradiance changes and the two strong eruptions, the question remains if other natural forcings contributed to the reconstructed early 19th-century cooling.

One possible source is small-to-moderate volcanic eruptions that are commonly not included in climate model simulations of the 19th century (e.g., Jungclaus et al., 2017) even though their possible impacts have been noticed one century ago (Humphreys, 1913). Solomon et al. (2011) point out that background stratospheric aerosol was variable and not constant over the past decades, even when the major volcanic eruptions were absent. Schmidt et al. (2018) show that small-to-moderate size eruptions occurred frequently over the last 50 years, causing small but significant temporary surface cooling. It has been suggested that small-to-moderate eruptions should be included in historical simulations (Mills et al., 2016; Vernier et al., 2011). For example, a faster rate of global warming was found in simulations of the first 15 years of the 21st century if volcanic eruptions since the year 2000 were excluded (Fyfe et al., 2013; Ridley et al., 2014; Santer et al., 2014; Schmidt et al., 2018). The main reason why small-to-moderate eruptions are not included in paleoclimate simulations is the difficulty of securely discriminating volcanic sulfur signals in ice cores which are of comparable strength to the background noise. Hence, accurate detection and quantification of sulfate aerosol forcing are more challenging for small-to-moderate volcanic eruptions (Cole-Dai, 2010).

For times before satellite observations, volcanic activity and the associated radiative forcing are traditionally reconstructed from the polar ice-sheets of Greenland and Antarctica (Gao et al., 2008; Sigl et al., 2015, 2022; Toohey & Sigl, 2017). Volcanic sulfuric acid aerosols are deposited and archived on these ice sheets. These can be detected and dated as characteristic signals in glaciochemical measurements of ice-cores as acid or sulfates. Since there are other sources of sulfate besides volcanic eruptions (e.g., from marine biogenic emissions), outlier detection algorithms are typically applied to isolate and quantify the volcanic fractions (Cole-Dai, 2010). The respective thresholds are usually chosen rather conservatively (to minimize false positives) and often applied to annually averaged data to counteract any negative influence from marine biogenic sulfate emissions, which have a very pronounced annual cycle. As a result, only very strong sulfate anomalies that are depicted in the ice-core volcanic proxies over a span of 1–3 years are used in reconstructions (Figures S1–S3 in Supporting Information S1, panels a and b). For example, the most recent reconstruction based on a network of ice-cores from Greenland and Antarctica (Toohey & Sigl, 2017) identifies only 6 eruptions between 1791 and 1830 CE, including strong eruptions in 1809, 1815, 1831, and 1835. Within this time window, at least 60 eruptions occurred with volcanic explosivity index (VEI) ≥ 3 , including 17 with VEI ≥ 4 (Global Volcanism Program, 2013), a strength that typically produces measurable climate signals (Schmidt et al., 2018). Here, we adopt a new detection method of volcanic signals in ice-cores to provide additional information also for smaller volcanic eruptions for which the detectable sulfate deposition lasted only for months instead of years.

To understand how important these small-to-moderate eruptions are in the early 19th-century climate and whether they could explain the mismatch between model simulations and temperature reconstructions, we have performed three large ensemble simulations experiments: with no volcanic forcing; with the volcanic forcing suggested in the protocol for the past1000 experiment of the Paleoclimate Modeling Intercomparison Project—Phase 4 (PMIP4 past1000, Jungclaus et al., 2017); and with radiative forcing estimates for small-to-moderate eruptions during the early 19th century that were identified here (for the first time) based on the new ice-core reconstruction.

2. Methods and Data

2.1. New Volcanic Forcing Including Small-To-Moderate Eruptions

We use new high time-resolution measurements (D4i; McConnell, 2016) of the D4 ice-core (McConnell et al., 2007) in Greenland (71.40°N, 43.08°W; 41 cm ice equivalent year⁻¹), drilled at a site with twice the snow accumulation rate compared to ice-cores previously used for the PMIP4 volcanic reconstructions (Toohey & Sigl, 2017). At 2,713 m altitude, the site is well-suited for recording stratospheric volcanic sulfate deposition since it is only minimally affected by tropospheric marine sulfate emissions. Owing to the high accumulation rate this ice-core dated through annual-layer counting is believed to have no age uncertainty (McConnell et al., 2007). Details on the used ice-core proxies and methodologies of detection and quantification of volcanic sulfate deposition from small-to-moderate past volcanic eruptions (1732–1900) and their climate forcing potential are described in Supporting Information S1 (Figures S1–S6).

Twelve new small-to-moderate eruptions are detected in the D4i record over the experiment period (1791–1830) and 35 in total over the entire ice-core data period (1733–1895; Figures S1–S3 in Supporting Information S1).

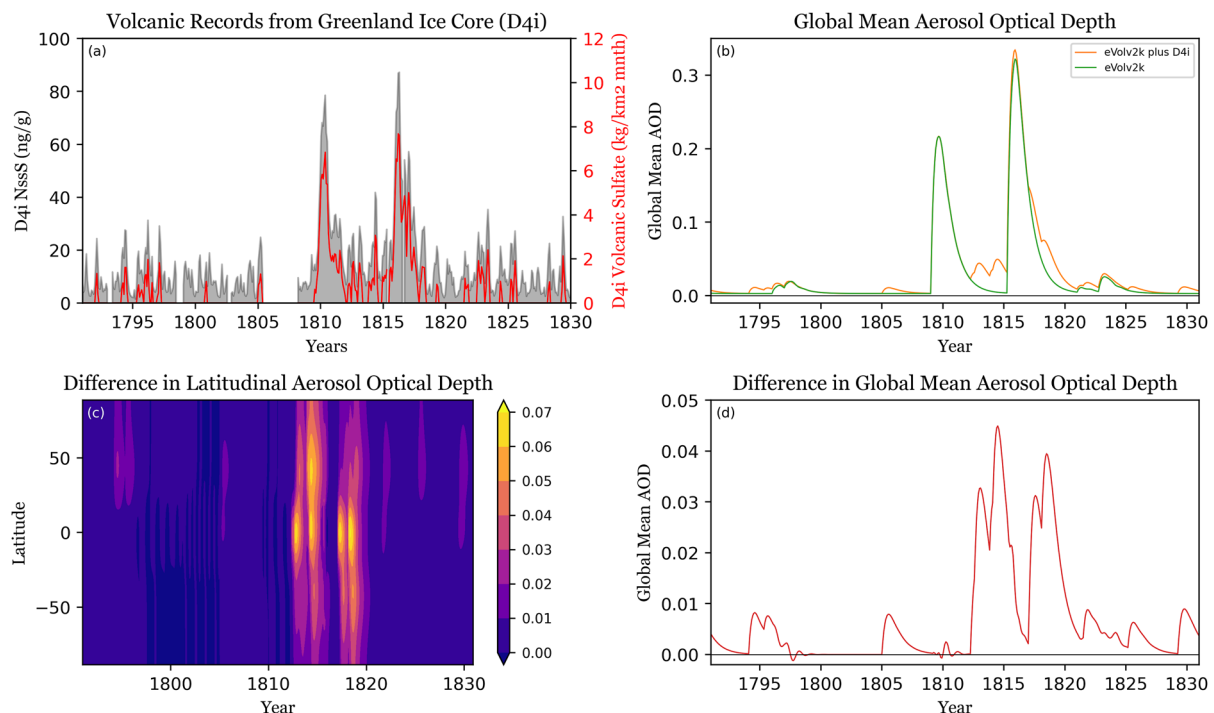


Figure 1. (a) Non-sea-salt sulfur (NssS) and Volcanic Sulfate from ice-core data of the new D4i ice-core over 1791–1830. (b) Global mean SAOD of the eVolv2k with and without the new D4i volcanic forcing over 1735–1875. (c) Zonal average and (d) Difference in global mean SAOD with and without including the new D4i volcanic forcing over 1791–1830.

Reconstructed sulfur injections for these events are between 0.3 and 2.6 TgS (Figure S5 in Supporting Information S1); comparable in strength to the VEI = 4 eruptions of Kasatochi 2008, Sarychev 2009 or Nabro 2011 (Carn et al., 2016). Some of the detected signals, dated to 1812, 1812, 1813, 1814, 1817, and 1818, are strikingly consistent with eruption ages of known moderate (VEI = 4) eruptions (i.e., Soufriere St. Vincent, and Awu in 1812; Suwanosejima in 1813; Mayon in 1814; Raung in 1817; Colima 1818) (Figure 1a; Figure S4 in Supporting Information S1) and we assign these signals to these eruptions (Figure S6 in Supporting Information S1). For sulfate signals that cannot be matched to a known eruption, since we cannot determine whether the source is tropical or extratropical, the sulfate deposition is split into components hypothetically associated with potential tropical and extratropical sources based on the fraction of source regions in the eVolv2k ice core reconstruction. The new eruptions are merged with eVolv2k (Toohey & Sigl, 2017), and the resulting eruption list is used as input to the Easy Volcanic Aerosol (EVA) forcing generator (Toohey et al., 2016) to derive an updated estimate of stratospheric aerosol optical depth (SAOD) over the experiment period (Figures 1b–1d) for the model. Over the 1791–1830 period, the average SAOD increased from 0.030 to 0.037, an increase of 24%, due to the inclusion of small-to-moderate events. In the revised reconstruction, the decade between 1809 and 1818 includes eight moderate (VEI = 4) to very large eruptions (VEI ≥ 6), which together emitted close to 60 TgS in the stratosphere.

2.2. Model

We use the low-resolution version of the Max-Planck-Institute Earth-System-Model (MPI-ESM1.2-LR, Mauritsen et al., 2019), one of the two MPI-ESM reference versions used in the Coupled Model Intercomparison Project Phase 6 (CMIP6; Eyring et al., 2016). The model consists of four components: the atmospheric general circulation model ECHAM6 (Stevens et al., 2013), the ocean-sea ice model MPIOM (Jungclaus et al., 2013), the land component JSBACH (Reick et al., 2013) and the marine biogeochemistry model HAMOCC (Ilyina et al., 2013). The model has an atmospheric horizontal resolution of T63 (~200 km) and uses 47 vertical levels up to 0.01 hPa (with 13 model levels above 100 hPa). In the ocean, a horizontal GR15 configuration is used with a nominal resolution of 1.5° around the equator and 40 vertical levels. The MPI-ESM1.2-LR has been successfully used to study the past climate (Van Dijk et al., 2022) and widely tested in the context of the climate of the early 19th century (Fang et al., 2021; Timmreck et al., 2021; Zanchettin et al., 2019).

2.3. Experiments

Three experiments from 1791 to 1830 are conducted in this study: Large-Only, Small-Included, and No-Volcano. The Large-Only experiment has the same setting as the MPI-ESM CMIP6/PMIP4 past2k simulation (van Dijk et al., 2022) and uses the EVA forcing for the aerosol optical properties from strong eruptions (Figure 1b). The Small-Included experiment changes the volcano forcing to eVolv2k plus D4i (Figure 1b), which includes the small-to-moderate volcanic eruptions as described in Section 2.2 and Supporting Information S1. The No-Volcano experiment uses the climatological SAOD forcing without volcanoes and is used as a control simulation for calculating anomalies. All experiments have 20 ensemble members generated from simulations branched at the year 1771 of the MPI-ESM past2k simulation and run for another 20 years (1771–1790) for distinct ocean states (Fang et al., 2022).

2.4. Data

Besides the model simulations, proxy and station data are used in this study. Three proxy-based reconstructions (Büntgen et al., 2021; Guillet et al., 2017; Wilson et al., 2016) of northern hemisphere extratropical summer land surface temperature are used. And one station-based reconstruction (Brönnimann, Allan, et al., 2019) on the regional climates is also included.

3. Results

As shown in Figure 1a; Figures S1–S4 in Supporting Information S1, twelve small-to-moderate eruptions are identified from the new volcanic forcing reconstruction over the experiment period (1791–1830). Figures 1b and 1c illustrate the global mean SAOD of the eVolv2k and the eVolv2k plus D4i forcing reconstructions, as well as their difference over the 1733–1895 period. The small-to-moderate eruptions spread over the experiment period and a set of relatively large eruptions is concentrated over 1812–1820. These cumulative eruptions contribute to the largest amount of SAOD changes within a decade over the entire ice-core period.

The near-surface air temperature (SAT) anomalies from simulations of the Large-Only and Small-Included experiments are shown in Figure 2. As expected, the isolated small-to-moderate eruptions outside 1812–1820 do not yield significant cooling in the global mean, as their signal is hidden in the internal variability. In contrast, during 1812–1820, the immediate responses from the six nearly consecutive small-to-moderate eruptions (Figure 1) can be found with the small spikes right after the eruptions (Figure 2a). The 1812–1820 small-eruption cluster contributes significantly to the global surface cooling by ~ 0.07 K for 10 years (averaged over 1814–1824) along with the large 1809 and 1815 eruptions that induce alone a roughly 5–10 times larger cooling (Figure 2a). The two large eruptions alone produce an immediate strong cooling, which rapidly recovers toward the climatology as the SAOD decreases, and only relatively small cold anomalies remain after the direct forcing influence has vanished.

The four small-to-moderate eruptions after 1809 and before 1815 Tambora provide additional cooling when the cooling induced by the 1809 eruption weakens. This slower recovery toward climatology sets a significantly colder climate before the 1815 Tambora eruption. This colder precondition of 1815 eruption, however, does not maintain at the cooling peak of the 1815 Tambora eruption, which may be due to the direct constraint of its strong radiative responses. The two small-to-moderate eruptions of Raung in 1817 and Colima in 1818 then again lead to significantly stronger cooling in the aftermath of the 1815 Tambora eruption. The effect of these small eruptions largely decreases as the SAOD is dampened and is no longer significant in 1825.

Next, we compare our results with the reconstructions of summer northern extra-tropical land temperature (Figure 2b). In both reconstructions, the cooling is smoothly developed after 1809, reaches its peak around 1816, and slowly recovers toward climatology. This smooth development of cooling before 1816 in the reconstructions is different from the simulations, which show a strong spike due to the 1809 eruption. The 1815 Tambora eruption is clearly visible in the reconstructions with a peak cooling of more than 1 K. We note that the two reconstructions show a warmer state before 1808 but have similar strength of maximum cooling at the peak for the 1815 Tambora eruption, indicating a distinct magnitude of the cooling. The cooling response to the Tambora eruption is much stronger in the simulations with an even stronger cooling in the Small-Included simulations.

The simulated slower recovery of temperature anomalies after 1816 in the Small-Included simulations is more consistent with the reconstructions. The small-to-moderate eruptions in 1812–1820 therefore help explain partly

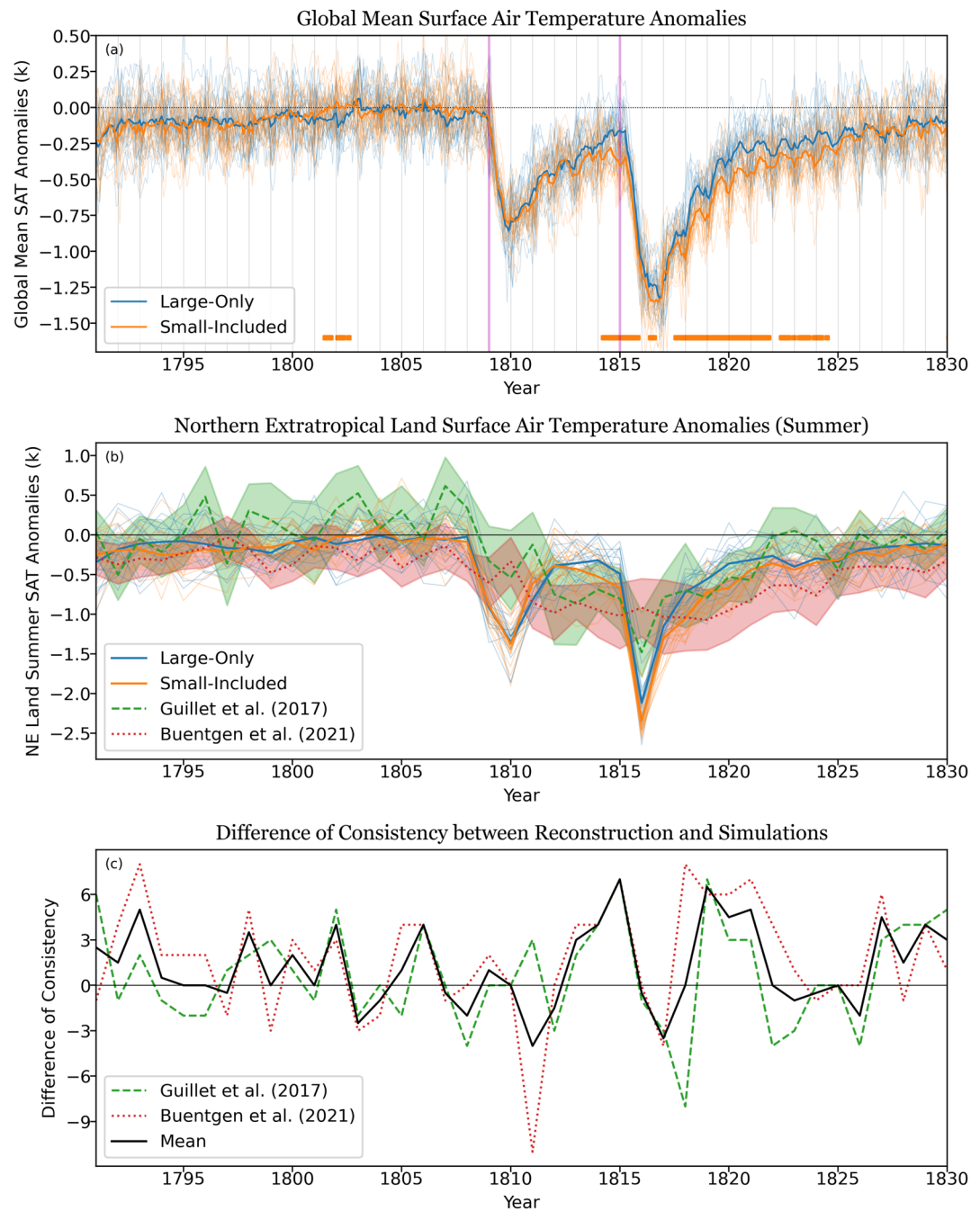


Figure 2. (a) Global mean surface air temperature anomalies of the Large-Only and Small-Included experiments. The gray lines are the January of each year and magenta for 1809 and 1815. The orange rectangles indicate the month has a significant difference between the two experiments by the student-*t* test with a 5% significance level over 20 ensembles. (b) Northern extratropical land surface air temperature but with proxy-based reconstructions (green dashed: Guillet et al., 2017; red dotted: Büntgen et al., 2021) and the shading indicates uncertainties. (c) The difference between the number of ensemble members having values within the reconstruction spread for the Small-Included and Large-Only experiments. The black line is the mean of two different reconstructions.

the slow return with additional cooling, though significant responses are only found until 1821. If we count the ensemble members that have values within the reconstruction spread, we find that, on average over the two reconstructions, the Small-Included have 5–6 more ensemble members than the Large-Only experiment right after the two large eruptions (Figure 2c). This entails that the small-to-moderate eruptions can help explaining

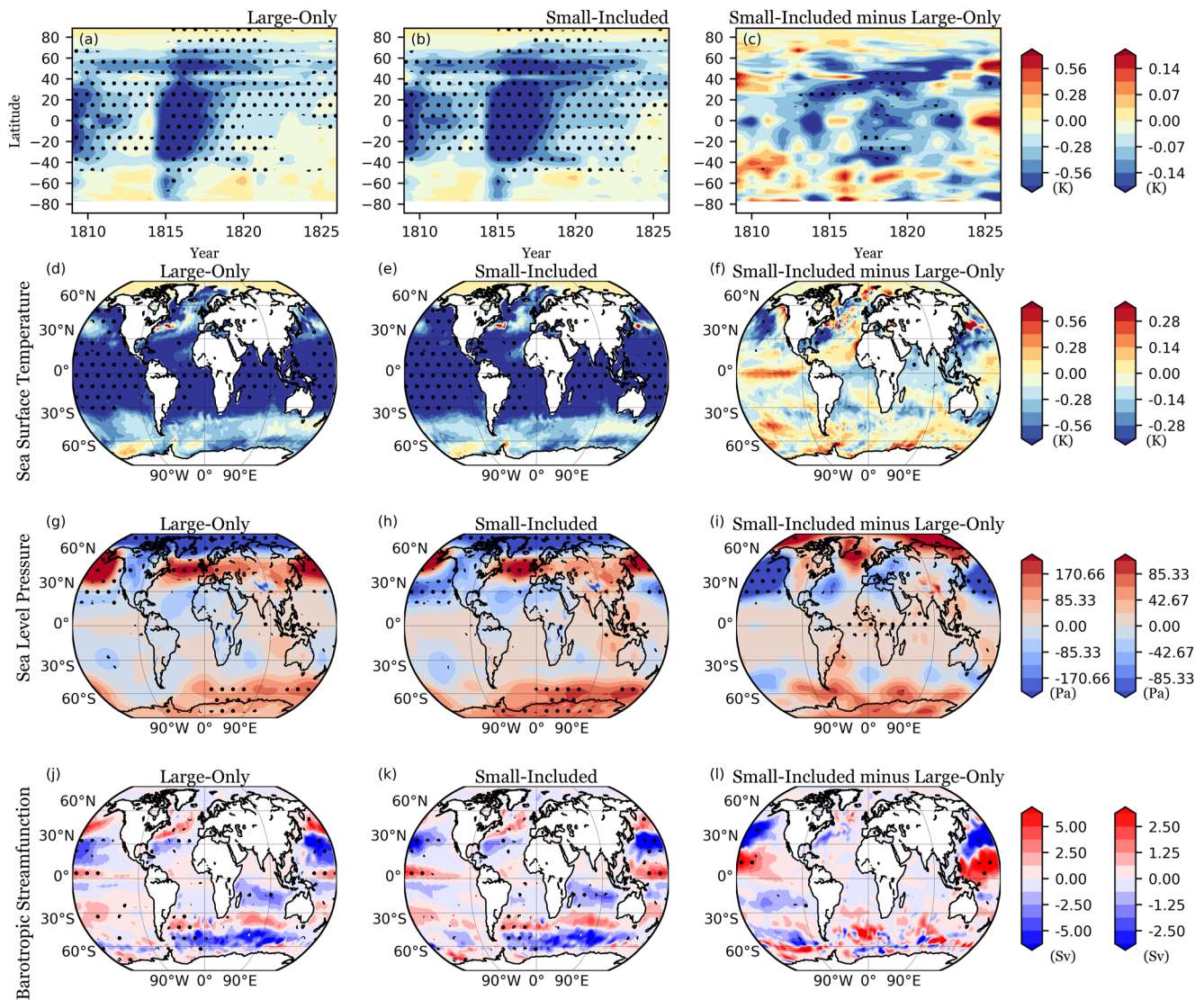


Figure 3. (a) Hovmöller plot for zonal mean winter SST anomaly (K) for the Large-Only experiment, (b) Small-Included, and (c) Small-Included minus Large-Only. (d) Winter composite of SST anomalies over 1815–1817 for the Large-Only experiment, (e) Small-Included, and (f) Small-Included minus Large-Only. (g–i) are sea level pressure anomalies (Pa). (j–l) are oceanic barotropic streamfunction anomalies (Sv). The black dots illustrate the significance with respect to the NoVolcano experiment for the Large-Only and the Small-Included experiment for the two left columns. And *t*-test significance is considered between the two experiments for the right most column.

the long-lasting cooling after the two strong eruptions. It should be noted that uncertainty remains in reconstructions of both surface temperature and forcing data. Due to the biological memory, tree-ring based reconstructions cause a delayed response to temperature variations (Zhu et al., 2020). Besides small-to-moderate eruptions, reconstructed solar and volcanic forcing with different methods may also reflect substantial uncertainties (Lücke et al., 2019, 2023).

Then, we investigate the dynamical interactions between the surface responses of small-to-moderate and large eruptions since Fang et al. (2022) have shown that the temperature responses to solar irradiance changes and volcanic forcing may not be additive on the regional scale due to their dynamical interactions. Figures 3a–3c shows the Hovmöller diagram of the zonal mean sea surface temperature (SST) anomalies over 1808–1830. After the first two small-to-moderate eruptions in 1812 (Soufriere St. Vincent, and Awu), the SST cooling is only found in the tropical Pacific, and no apparent cooling occurs in the northern extra-tropics even though a small signature of cooling remains at around 20°N. The third (1813 Suwanosejima) and fourth (1814 Mayon) eruptions lead to cooling not only in the tropics but also in the northern extra-tropics since the 1813 eruption is

identified as a northern extratropical eruption. As a result, the cooling around 20°N from the first two eruptions is combined with the cooling from the third and fourth eruptions before the 1815 Tambora. The cooling at 20°N, then, slowly propagates to higher latitudes over about for 10 years. During the propagation, the fifth and sixth small-to-moderate eruptions (Raung in 1817; Colima 1818) further enhance the cooling and sustain the northward propagation of anomalies. Significant differences between the Large-Only and Small-Included experiments can be found in the tropics and along the propagation mainly between 1817 and 1820. Compared to the eruptions before 1815 having significant cooling after the third eruption, significant cooling is found after 1815 until 1824. As the small-to-moderate eruptions before and after 1815 have similar AOD values, individual events should not cause significant cooling responses until 1820. This entails that the colder initial conditions for the 1815 Tambora set by the small-to-moderate eruptions before 1815 may lead to a stronger cooling for the eruptions after Tambora.

To understand why the additional cooling is first found within the tropics and further propagates northward, we investigate the dynamical influences of the 1815 Tambora eruption on the responses to the cluster of small-to-moderate eruptions. Figures 3d–3l show the SST, sea level pressure (SLP), and oceanic barotropic streamfunction responses after the 1815 eruption. The responses indicate a southward shift of the gyres in the northern hemisphere related to a southward shift of the westerlies (Figures S7g and S7h in Supporting Information S1) for both Large-Only and Small-Included experiments; however, no significant difference in ocean circulation is found between the two experiments even though the SLP exhibits significant difference (Figure 3i). Also, due to a southward shift of western boundary currents (Figures S7a and S7b in Supporting Information S1) by the Tambora, a weakening of northward heat transport (Figures S7d and S7e in Supporting Information S1) is found at the surface but not for the entire ocean column (Figures S7j and S7k in Supporting Information S1) for both experiments. As a result, we interpret that the additional cooling from the cluster of small-to-moderate eruptions remains confined to the tropics because the Tambora weakens the ocean circulation and the cooling extends to higher latitudes as the gyres recover (Figure S8 in Supporting Information S1). That is, the distribution over time of additional cooling from the small-to-moderate eruptions can be influenced by the dynamical responses triggered by the strong 1815 Tambora.

We further investigate the regional responses to the eruptions and compare them with the station-based reconstruction since the small eruptions may lead to a unique response in each region as the additional cooling is transported to the north. Figure 4 shows the summer land surface air temperature of the experiments in the east U.S. and west, east, north, south, and central Europe defined by the reconstruction from Brönnimann, Allan, et al. (2019). From the simulations, we can see that the regions individually feature only sporadically significant responses to the small-to-moderate eruptions, but as a whole reveal a possible signature of the northward propagating cooling: the east USA has more cooling before 1815 when the cool water remains in the western Pacific, and western Europe has significant cooling after 1817, when the cooling propagates to the eastern north Atlantic. On the other hand, the station data have large variability in all regions and do not allow us to conclude whether the small-to-moderate eruptions can explain the regional difference. Especially the record from western Europe shows a strong positive overshoot after 1815 while the simulation shows significant cooling for several years. That is, even though the peak cooling of Tambora in individual regions are comparable to the simulations, the impacts of small-to-moderate eruptions cannot be identified from the station-based reconstruction. We also investigate the proxy-based reconstruction in eastern and western North America and EuroAsia from the N-TREND with a larger region concerned (Figure S9 in Supporting Information S1; Wilson et al., 2016). Similar to the station-based data, large discrepancies are found between reconstructions and simulations outside the Tambora event. Therefore, even though all regions for the simulations show significant responses after 1814, we cannot conclude that small volcanoes help explain the long-lasting cooling after Tambora. If we compare the histogram of summer land surface air temperature over 1808–1820 of the Small-Included and Large-Only experiments in regions with the station-based data (Figure S10 in Supporting Information S1), we can see that the small-to-moderate eruptions lower the mean but have limited effects on the tails. That is, the small-to-moderate eruptions has limited enhancement on the maximum regional cooling by the two large eruptions, but instead contribute to regional cooling when the impacts of the two large eruptions weaken.

4. Summary and Discussion

In this study, we introduce a new volcanic forcing data set calculated from the new high-time-resolution measurements of the D4 ice-core in Greenland and show that the newly identified small-to-moderate eruptions can

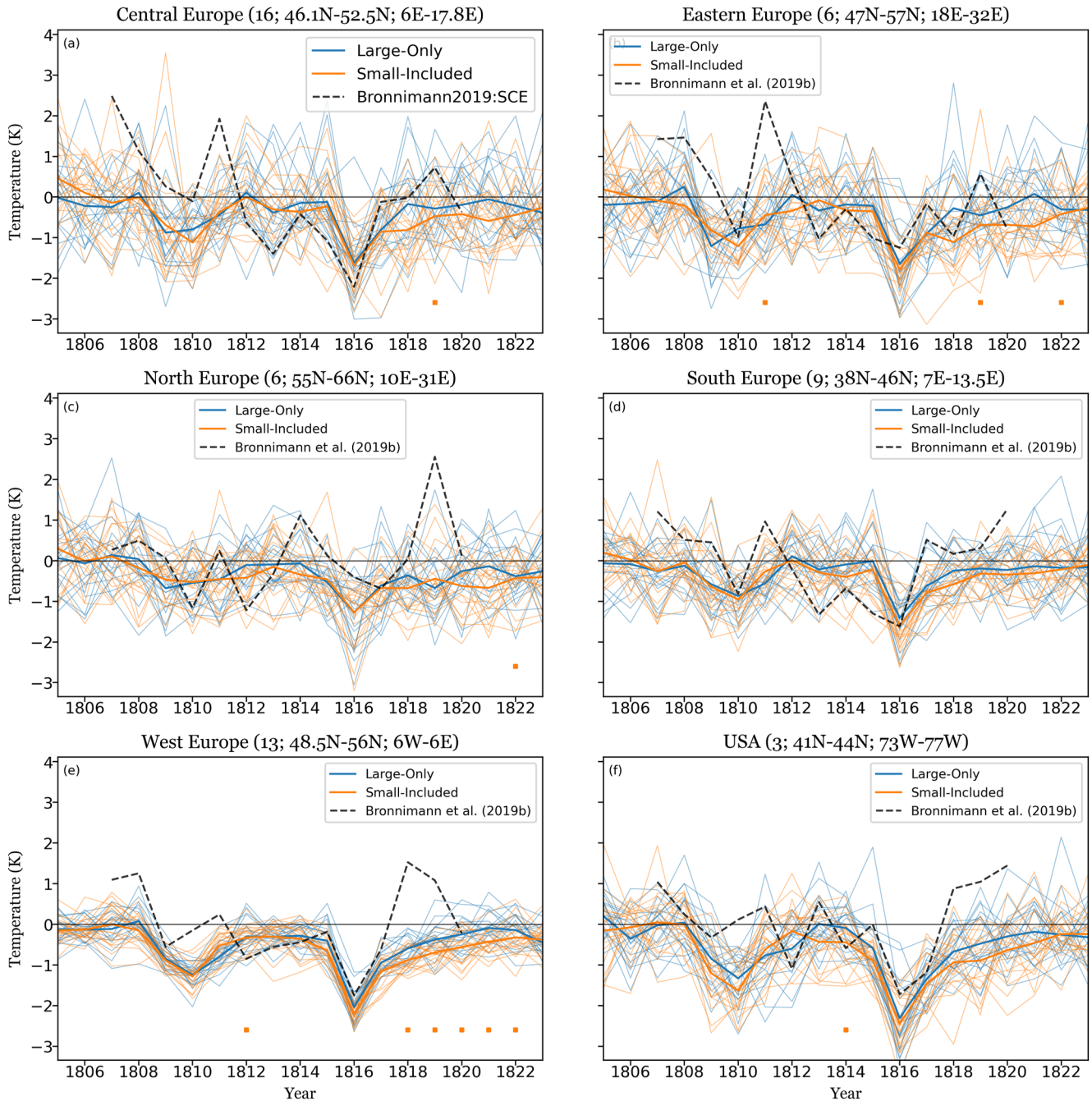


Figure 4. The summer land surface air temperature anomalies over (a) Central, (b) East, (c) North, (d) South, (e) West Europe, and (f) USA of the Large-Only and Small-Included experiment with the station-based reconstruction of each region defined by Brönnimann, Allan, et al. (2019). The number of stations and the boxes of regions are shown in the title of each plot.

significantly contribute to the early 19th century cooling along with the two large eruptions: 1809 unidentified and 1815 Tambora.

The high altitude and high snow accumulation rates at this ice-core site allow us to identify excess sulfuric acid deposits in the precisely dated and monthly resolved data, which often closely match dates of historical moderate eruptions (i.e., VEI = 4) in both the tropics and mid-latitudes of the Northern Hemisphere. We consequently assigned these sulfur anomalies to historical volcanic eruptions (or distributed sulfur injections into default latitudes if no plausible eruption candidate was apparent) and estimated stratospheric sulfur injections

and subsequent changes in SAOD. Considerable uncertainties exist in both source attribution and sulfur emission estimates for these new identified eruptions, but the reconstructed sulfur injections (up to 3 TgS) are well within the range of those from comparably sized volcanic eruptions obtained by remote sensing (Carn et al., 2016).

Significant additional surface cooling is found not only during the small-to-moderate eruptions but occurs also for 5 years following the volcanic cluster (until 1825). This is because the additional cooling from small-to-moderate eruptions is distributed by the ocean circulation changes that are determined by the two large eruptions. After the two large eruptions, the cooling from the small-to-moderate eruptions persists in the tropics due to the weakening of the Kuroshio and Gulf Stream, and the cooling then propagates to the northern extratropics which results in a long-lasting cooling response. Similar regional impacts from relatively small forcing during large eruptions are also found when comparing the additional effect of changes in solar irradiance (Fang et al., 2022). That is, this novel oceanic mechanism indicates that the responses to relatively small forcing (small eruptions and solar irradiance) may be influenced by the stronger long-lasting impacts from the large forcing (large eruptions), which needs to be further understood in different models.

We also investigated the consistency between the reconstructions and our simulations, as small eruptions have recently been suggested to be included in future climate projections (Chim et al., 2023) but have not been included in pre-industrial simulations. For the large-scale anomalies, the small-to-moderate eruptions help explaining the long-lasting cooling after the two strong eruptions found in the reconstructions. For regional scales, the proxy- and station-based reconstructions exhibit a large variability, which prevents identifying regional impacts found in simulations. Comparing with the solar forcing, the cooling contribution of small-to-moderate eruptions is between the two solar forcing considered in Fang et al. (2022). To summarize, from the MPI-ESM simulations, the cooling contribution to the 19th-century is mainly from the two strong volcanic (1809 and 1815) eruptions and the small-to-moderate eruptions and solar irradiance may both contribute to the long-lasting cooling after the strong eruptions.

Data Availability Statement

The Python codes for generating the figures, the processed data of the variables from the simulations, and the SAOD forcing of eVolv2k plus D4i can be accessed at Zenodo (Fang, 2023). Ice-core aerosol records can be accessed from the NSF Arctic Data Center (D4; McConnell, 2016), at PANGAEA (NEEM-2011-S1; Sigl & McConnell, 2022) and here: (NGRIP, Plummer, 2012). Reconstructed volcanic sulfate deposition from D4i can be accessed at PANGAEA (Sigl & McConnell, 2023); the combined eVolv2k plus D4i volcanic eruption catalog for 1733–1895 CE and reconstructed stratospheric sulfur injection can be accessed at PANGAEA (Sigl et al., 2023).

References

- Anet, J. G., Muthers, S., Rozanov, E. V., Raible, C. C., Stenke, A., Shapiro, A. I., et al. (2014). Impact of solar versus volcanic activity variations on tropospheric temperatures and precipitation during the Dalton Minimum. *Climate of the Past*, 10(3), 921–938. <https://doi.org/10.5194/cp-10-921-2014>
- Brehm, N., Bayliss, A., Christl, M., Synal, H.-A., Adolphi, F., Beer, J., et al. (2021). Eleven-year solar cycles over the last millennium revealed by radiocarbon in tree rings. *Nature Geoscience*, 14(1), 10–15. <https://doi.org/10.1038/s41561-020-00674-0>
- Brönnimann, S., Allan, R., Ashcroft, L., Baer, S., Barriendos, M., Brázdil, R., et al. (2019). Unlocking pre-1850 instrumental meteorological records: A global inventory. *Bulletin of the American Meteorological Society*, 100(12), ES389–ES413. <https://doi.org/10.1175/BAMS-D-19-0040.1>
- Brönnimann, S., Franke, J., Nussbaumer, S. U., Zumbühl, H. J., Steiner, D., Trachsel, M., et al. (2019). Last phase of the Little Ice Age forced by volcanic eruptions. *Nature Geoscience*, 12(8), 650–656. <https://doi.org/10.1038/s41561-019-0402-y>
- Büntgen, U., Allen, K., Anchukaitis, K. J., Arseneault, D., Boucher, É., Bräuning, A., et al. (2021). The influence of decision-making in tree ring-based climate reconstructions. *Nature Communications*, 12(1), 3411. <https://doi.org/10.1038/s41467-021-23627-6>
- Carn, S. A., Clarisse, L., & Prata, A. J. (2016). Multi-decadal satellite measurements of global volcanic degassing. *Journal of Volcanology and Geothermal Research*, 311, 99–134. <https://doi.org/10.1016/j.jvolgeores.2016.01.002>
- Chim, M. M., Aubry, T. J., Abraham, N. L., Marshall, L., Mulcahy, J., Walton, J., & Schmidt, A. (2023). Climate projections very likely underestimate future volcanic forcing and its climatic effects. *Geophysical Research Letters*, 50(12), e2023GL103743. <https://doi.org/10.1029/2023GL103743>
- Cole-Dai, J. (2010). Volcanoes and climate. *WIREs Climate Change*, 1(6), 824–839. <https://doi.org/10.1002/wcc.76>
- Cole-Dai, J., Ferris, D., Lanciki, A., Savarino, J., Baroni, M., & Thiemens, M. H. (2009). Cold decade (AD 1810–1819) caused by Tambora (1815) and another (1809) stratospheric volcanic eruption. *Geophysical Research Letters*, 36(22), L22703. <https://doi.org/10.1029/2009GL040882>
- Eyring, V., Bony, S., Meehl, G. A., Senior, C. A., Stevens, B., Stouffer, R. J., & Taylor, K. E. (2016). Overview of the Coupled Model Inter-comparison Project Phase 6 (CMIP6) experimental design and organization. *Geoscientific Model Development*, 9(5), 1937–1958. <https://doi.org/10.5194/gmd-9-1937-2016>

Acknowledgments

We thank two anonymous reviewers for their valuable comments and Dr. Jalihal Chetankumar who gave valuable comments on an earlier version of this paper. The research for SWF is funded by the German Federal Ministry of Education and Research (BMBF), research programme “ROMIC-II, ISOVIC” (FKZ: 01LG1909B). CT acknowledges support to this research by the Deutsche Forschungsgemeinschaft Research Unit VolImpact (FOR2820, Grant 398006378) within the project VolClim (TI 344/2-1). MS acknowledges funding from the European Research Council (ERC) under the European Union’s Horizon 2020 research and innovation programme (Grant agreement No 820047). The computations, analysis and model data storage were mainly performed on the computer of the Deutsches Klima Rechenzentrum (DKRZ) using resources granted by its Scientific Steering Committee (WLA) under project ID bb1171. We acknowledge the World Climate Research Programme’s Working Group on Coupled Modeling, which is responsible for PMIP. The analyses were performed using Python. Open Access funding enabled and organized by Projekt DEAL.

- Fang, S.-W. (2023). The role of small to moderate volcanic eruptions in the early 19th century climate [Dataset]. Zenodo. <https://doi.org/10.5281/zenodo.8017389>
- Fang, S.-W., Khodri, M., Timmreck, C., Zanchettin, D., & Jungclaus, J. (2021). Disentangling internal and external contributions to Atlantic multidecadal variability over the past millennium. *Geophysical Research Letters*, *48*(23), e2021GL095990. <https://doi.org/10.1029/2021GL095990>
- Fang, S.-W., Timmreck, C., Jungclaus, J., Krüger, K., & Schmidt, H. (2022). On the additivity of climate responses to the volcanic and solar forcing in the early 19th century. *Earth System Dynamics*, *13*(4), 1535–1555. <https://doi.org/10.5194/esd-13-1535-2022>
- Fyfe, J. C., Gillett, N. P., & Zwiers, F. W. (2013). Overestimated global warming over the past 20 years. *Nature Climate Change*, *3*(9), 767–769. <https://doi.org/10.1038/nclimate1972>
- Gao, C., Robock, A., & Ammann, C. (2008). Volcanic forcing of climate over the past 1500 years: An improved ice-core-based index for climate models. *Journal of Geophysical Research*, *113*(D23), D23111. <https://doi.org/10.1029/2008JD010239>
- Global Volcanism Program. (2013). Global volcanism program. Volcanoes of the World, v. 4.11.0 (08 Jun 2022) [Weblink]. <https://doi.org/10.5479/si.GVP.VOTW4-2013>
- Guillet, S., Corona, C., Stoffel, M., Khodri, M., Lavigne, F., Ortega, P., et al. (2017). Climate response to the Samalás volcanic eruption in 1257 revealed by proxy records. *Nature Geoscience*, *10*(2), 123–128. <https://doi.org/10.1038/ngeo2875>
- Humphreys, W. J. (1913). Volcanic dust as a factor in the production of climatic changes. *Journal of the Washington Academy of Sciences*, *3*(13), 365–371.
- Ilyina, T., Six, K. D., Segschneider, J., Maier-Reimer, E., Li, H., & Núñez-Riboni, I. (2013). Global ocean biogeochemistry model HAMOCC: Model architecture and performance as component of the MPI-Earth system model in different CMIP5 experimental realizations. *Journal of Advances in Modeling Earth Systems*, *5*(2), 287–315. <https://doi.org/10.1029/2012MS000178>
- Jungclaus, J. H., Bard, E., Baroni, M., Braconnot, P., Cao, J., Chini, L. P., et al. (2017). The PMIP4 contribution to CMIP6—Part 3: The last millennium, scientific objective, and experimental design for the PMIP4 *past1000* simulations. *Geoscientific Model Development*, *10*(11), 4005–4033. <https://doi.org/10.5194/gmd-10-4005-2017>
- Jungclaus, J. H., Fischer, N., Haak, H., Lohmann, K., Marotzke, J., Matei, D., et al. (2013). Characteristics of the ocean simulations in the Max Planck Institute Ocean Model (MPIOM) the ocean component of the MPI-Earth system model. *Journal of Advances in Modeling Earth Systems*, *5*(2), 422–446. <https://doi.org/10.1002/jame.20023>
- Lücke, L. J., Hegerl, G. C., Schurer, A. P., & Wilson, R. (2019). Effects of memory biases on variability of temperature reconstructions. *Journal of Climate*, *32*(24), 8713–8731. <https://doi.org/10.1175/JCLI-D-19-0184.1>
- Lücke, L. J., Schurer, A. P., Toohey, M., Marshall, L. R., & Hegerl, G. C. (2023). The effect of uncertainties in natural forcing records on simulated temperature during the last millennium. *Climate of the Past*, *19*(5), 959–978. <https://doi.org/10.5194/cp-19-959-2023>
- Mauritsen, T., Bader, J., Becker, T., Behrens, J., Bittner, M., Brokopf, R., et al. (2019). Developments in the MPI-M Earth system model version 1.2 (MPI-ESM1.2) and its response to increasing CO₂. *Journal of Advances in Modeling Earth Systems*, *11*(4), 998–1038. <https://doi.org/10.1029/2018MS001400>
- McConnell, J. (2016). D4 continuous ice-core chemistry measurements below pore close off [Dataset]. Arctic Data Center. <https://doi.org/10.18739/A2JS9H808>
- McConnell, J. R., Arístarain, A. J., Banta, J. R., Edwards, P. R., & Simões, J. C. (2007). 20th-century doubling in dust archived in an Antarctic Peninsula ice-core parallels climate change and desertification in South America. *Proceedings of the National Academy of Sciences of the United States of America*, *104*(14), 5743–5748. <https://doi.org/10.1073/pnas.0607657104>
- Mills, M. J., Schmidt, A., Easter, R., Solomon, S., Kinnison, D. E., Ghan, S. J., et al. (2016). Global volcanic aerosol properties derived from emissions, 1990–2014, using CESM1(WACCM). *Journal of Geophysical Research: Atmospheres*, *121*(5), 2332–2348. <https://doi.org/10.1002/2015JD024290>
- Owens, M. J., Lockwood, M., Hawkins, E., Usoskin, I., Jones, G. S., Barnard, L., et al. (2017). The Maunder minimum and the Little Ice Age: An update from recent reconstructions and climate simulations. *Journal of Space Weather and Space Climate*, *7*, A33. <https://doi.org/10.1051/swsc/2017034>
- PAGES 2k Consortium. (2019). Consistent multidecadal variability in global temperature reconstructions and simulations over the Common Era. *Nature Geoscience*, *12*(8), 643–649. <https://doi.org/10.1038/s41561-019-0400-0>
- Plummer (2012). Sulphate data from the NGRIP ice cores [Dataset]. Centre for Ice and Climate. https://www.iceandclimate.nbi.ku.dk/data/2012-12-03_NGRIP_SO4_5cm_Plummer_et_al_CP_2012.txt
- Reichen, L., Burgdorf, A.-M., Brönnimann, S., Franke, J., Hand, R., Valler, V., et al. (2022). A decade of cold Eurasian winters reconstructed for the early 19th century. *Nature Communications*, *13*(1), 2116. <https://doi.org/10.1038/s41467-022-29677-8>
- Reick, C. H., Raddatz, T., Brovkin, V., & Gayler, V. (2013). Representation of natural and anthropogenic land cover change in MPI-ESM. *Journal of Advances in Modeling Earth Systems*, *5*(3), 459–482. <https://doi.org/10.1002/jame.20022>
- Ridley, D. A., Solomon, S., Barnes, J. E., Burlakov, V. D., Deshler, T., Dolgii, S. I., et al. (2014). Total volcanic stratospheric aerosol optical depths and implications for global climate change. *Geophysical Research Letters*, *41*(22), 7763–7769. <https://doi.org/10.1002/2014GL061541>
- Santer, B. D., Bonfils, C., Painter, J. F., Zelinka, M. D., Mears, C., Solomon, S., et al. (2014). Volcanic contribution to decadal changes in tropospheric temperature. *Nature Geoscience*, *7*(3), 185–189. <https://doi.org/10.1038/ngeo2098>
- Schmidt, A., Mills, M. J., Ghan, S., Gregory, J. M., Allan, R. P., Andrews, T., et al. (2018). Volcanic radiative forcing from 1979 to 2015. *Journal of Geophysical Research: Atmospheres*, *123*(22), 12491–12508. <https://doi.org/10.1029/2018JD028776>
- Schurer, A. P., Tett, S. F. B., & Hegerl, G. C. (2014). Small influence of solar variability on climate over the past millennium. *Nature Geoscience*, *7*(2), 104–108. <https://doi.org/10.1038/ngeo2040>
- Sigl, M., Abram, N. J., Gabrieli, J., Jenk, T. M., Osmont, D., & Schwikowski, M. (2018). 19th century glacier retreat in the Alps preceded the emergence of industrial black carbon deposition on high-alpine glaciers. *The Cryosphere*, *12*(10), 3311–3331. <https://doi.org/10.5194/tc-12-3311-2018>
- Sigl, M., & McConnell, J. R. (2022). NEEM-2011-S1 ice-core aerosol record (conductivity, NH₄, NO₃, BC, acidity, Na, Mg, S, Ca, Mn, Sr, Ce) in NW-Greenland at 2 cm resolution from 86-1997 CE on the annual-layer counted NS1-2011 chronology [Dataset]. PANGAEA. <https://doi.org/10.1594/PANGAEA.940553>
- Sigl, M., & McConnell, J. R. (2023). D4i Greenland ice-core non-sea-salt sulfur concentrations and calculated volcanic sulfate deposition (1733–1900 CE) [Dataset]. PANGAEA. <https://doi.org/10.1594/PANGAEA.960977>
- Sigl, M., McConnell, J. R., & Toohey, M. (2023). Volcanic stratospheric sulfur injection between 1733 and 1895 CE based on the eVolV2k-plus-D4i ice-core eruption catalogue [Dataset]. PANGAEA. <https://doi.org/10.1594/PANGAEA.960975>
- Sigl, M., Toohey, M., McConnell, J. R., Cole-Dai, J., & Severi, M. (2022). Volcanic stratospheric sulfur injections and aerosol optical depth during the Holocene (past 11 500 years) from a bipolar ice-core array. *Earth System Science Data*, *14*(7), 3167–3196. <https://doi.org/10.5194/essd-14-3167-2022>

- Sigl, M., Winstrup, M., McConnell, J. R., Welten, K. C., Plunkett, G., Ludlow, F., et al. (2015). Timing and climate forcing of volcanic eruptions for the past 2,500 years. *Nature*, *523*(7562), 543–549. <https://doi.org/10.1038/nature14565>
- Solomina, O. N., Bradley, R. S., Jomelli, V., Geirsdottir, A., Kaufman, D. S., Koch, J., et al. (2016). Glacier fluctuations during the past 2000 years. *Quaternary Science Reviews*, *149*, 61–90. <https://doi.org/10.1016/j.quascirev.2016.04.008>
- Solomon, S., Daniel, J. S., Neely, R. R., Vernier, J.-P., Dutton, E. G., & Thomason, L. W. (2011). The persistently variable “background” stratospheric aerosol layer and global climate change. *Science*, *333*(6044), 866–870. <https://doi.org/10.1126/science.1206027>
- Stevens, B., Giorgetta, M., Esch, M., Mauritsen, T., Cruieger, T., Rast, S., et al. (2013). Atmospheric component of the MPI-M Earth system model: ECHAM6. *Journal of Advances in Modeling Earth Systems*, *5*(2), 146–172. <https://doi.org/10.1002/jame.20015>
- Timmreck, C., Toohey, M., Zanchettin, D., Brönnimann, S., Lundstad, E., & Wilson, R. (2011). The unidentified eruption of 1809: A climatic cold case. *Climate of the Past*, *17*(4), 1455–1482. <https://doi.org/10.5194/cp-17-1455-2021>
- Toohey, M., & Sigl, M. (2017). Volcanic stratospheric sulfur injections and aerosol optical depth from 500 BCE to 1900 CE. *Earth System Science Data*, *9*(2), 809–831. <https://doi.org/10.5194/essd-9-809-2017>
- Toohey, M., Stevens, B., Schmidt, H., & Timmreck, C. (2016). Easy volcanic aerosol (EVA v1.0): An idealized forcing generator for climate simulations. *Geoscientific Model Development*, *9*(11), 4049–4070. <https://doi.org/10.5194/gmd-9-4049-2016>
- van Dijk, E., Jungclauss, J., Lorenz, S., Timmreck, C., & Krüger, K. (2022). Was there a volcanic-induced long-lasting cooling over the Northern Hemisphere in the mid-6th–7th century? *Climate of the Past*, *18*(7), 1601–1623. <https://doi.org/10.5194/cp-18-1601-2022>
- Vernier, J.-P., Thomason, L. W., Pommerehne, J.-P., Bourassa, A., Pelon, J., Garnier, A., et al. (2011). Major influence of tropical volcanic eruptions on the stratospheric aerosol layer during the last decade. *Geophysical Research Letters*, *38*(12), L12807. <https://doi.org/10.1029/2011GL047563>
- Wanner, H., Pfister, C., & Neukom, R. (2022). The variable European Little Ice Age. *Quaternary Science Reviews*, *287*, 107531. <https://doi.org/10.1016/j.quascirev.2022.107531>
- Wilson, R., Anchukaitis, K., Briffa, K. R., Büntgen, U., Cook, E., D’Arrigo, R., et al. (2016). Last millennium northern hemisphere summer temperatures from tree rings: Part I: The long term context. *Quaternary Science Reviews*, *134*, 1–18. <https://doi.org/10.1016/j.quascirev.2015.12.005>
- Zanchettin, D., Bothe, O., Graf, H. F., Lorenz, S. J., Luterbacher, J., Timmreck, C., & Jungclauss, J. H. (2013). Background conditions influence the decadal climate response to strong volcanic eruptions. *Journal of Geophysical Research: Atmospheres*, *118*(10), 4090–4106. <https://doi.org/10.1002/jgrd.50229>
- Zanchettin, D., Timmreck, C., Toohey, M., Jungclauss, J. H., Bittner, M., Lorenz, S. J., & Rubino, A. (2019). Clarifying the relative role of forcing uncertainties and initial-condition unknowns in spreading the climate response to volcanic eruptions. *Geophysical Research Letters*, *46*(3), 1602–1611. <https://doi.org/10.1029/2018GL081018>
- Zhu, F., Emile-Geay, J., Hakim, G. J., King, J., & Anchukaitis, K. J. (2020). Resolving the differences in the simulated and reconstructed temperature response to volcanism. *Geophysical Research Letters*, *47*(8), e2019GL086908. <https://doi.org/10.1029/2019GL086908>

References From the Supporting Information

- Bowen, H. J. M. (1979). *Environmental chemistry of the elements*. Academic Press.
- Pasteris, D. R., McConnell, J. R., & Edwards, R. (2012). High-resolution, continuous method for measurement of acidity in ice-cores. *Environmental Science & Technology*, *46*(3), 1659–1666. <https://doi.org/10.1021/es202668n>
- Plummer, C. T., Curran, M. A. J., van Ommen, T. D., Rasmussen, S. O., Moy, A. D., Vance, T. R., et al. (2012). An independently dated 2000-yr volcanic record from Law Dome, East Antarctica, including a new perspective on the dating of the 1450s CE eruption of Kuwae, Vanuatu. *Climate of the Past*, *8*(6), 1929–1940. <https://doi.org/10.5194/cp-8-1929-2012>
- Plunkett, G., Sigl, M., Schwaiger, H. F., Tomlinson, E. L., Toohey, M., McConnell, J. R., et al. (2022). No evidence for tephra in Greenland from the historic eruption of Vesuvius in 79CE: Implications for geochronology and paleoclimatology. *Climate of the Past*, *18*(1), 45–65. <https://doi.org/10.5194/cp-18-45-2022>
- Sigl, M., McConnell, J. R., Layman, L., Maselli, O., McGwire, K., Pasteris, D., et al. (2013). A new bipolar ice-core record of volcanism from WAIS Divide and NEEM and implications for climate forcing of the last 2000 years. *Journal of Geophysical Research: Atmospheres*, *118*(3), 1151–1169. <https://doi.org/10.1029/2012JD018603>
- Trautetter, F., Oerter, H., Fischer, H., Weller, R., & Miller, H. (2004). Spatio-temporal variability in volcanic sulphate deposition over the past 2 Kyr in snow pits and firn cores from Amundsenisen, Antarctica. *Journal of Glaciology*, *50*(168), 137–146. <https://doi.org/10.3189/172756504781830222>